Phytomedicine 22 (2015) 813–819

Contents lists available at ScienceDirect

Phytomedicine

journal homepage: www.elsevier.com/locate/phymed

Panax notoginseng saponins suppress radiation-induced osteoporosis by regulating bone formation and resorption

Du Wenxi [a,1], Duan Shufang [b,1], Yu Xiaoling [a], Yin Liming [a,*]

[a] *The First Affiliated Hospital of Zhejiang Chinese Medical University, Hangzhou, China*
[b] *The Second Affiliated Hospital of Zhejiang Chinese Medical University, Hangzhou, China*

ARTICLE INFO

Article history:
Received 20 January 2015
Revised 17 April 2015
Accepted 25 May 2015

Keywords:
Radiation
Total saponins of *Panax notoginseng* leaves
Antiosteoporotic
Osteoblast
Osteoclast

ABSTRACT

Background: While radiation-based therapies are effective for treating numerous malignancies, such treatments can also induce osteoporosis.
Purpose: We assessed the antiosteoporotic properties of total saponins extracted from the leaves of *Panax notoginseng* (LPNS) in a mouse model of radiation-induced osteoporosis and *in vitro*.
Study design/methods: The bone mineral densities, the marker of bone formation and resorption, and inflammatory factors were measured *in vivo*. Cell proliferation and differentiation were detected *in vitro*.
Results: The results showed that bone mineral densities in irradiated mice administered LPNS were significantly increased compared to those in irradiated mice which had not received LPNS. LPNS attenuated the inflammation caused by irradiation, and significantly increased blood serum AKP activity, the mRNA levels of RUNX2 and osteoprotegerin, and the numbers of CFU-Fs formed by bone marrow cells collected from irradiated mice. In contrast, LPNS decreased the numbers of osteoclast precursor cells ($CD117^+/RANKL^+$ cells and $CD71^+/CD115^+$ cells) and the mRNA levels of TRAP and ATP6i. These results suggest that LPNS functions as a negative regulator of bone resorption. *In vitro* assays showed that LPNS promoted the differentiation of bone marrow mesenchymal stem cells and mononuclear cells into osteoblasts and osteoclasts, respectively, but had no effect on osteoclast activation.
Conclusion: These results demonstrate that LPNS has significant antiosteoporotic activity, which may warrant further investigations concerning its therapeutic effects in treating radiation-induced osteoporosis.

Introduction

While radiotherapy is frequently used in cancer treatment, accumulated evidence indicates that radiation can also damage normal tissues (Zhao et al., 2009). Among various radiation-related complications, skeletal fractures are particularly compelling due to their high incidence and serious impact on a patient's quality of life (Williams and Davies, 2006). Moreover, overall fracture rates among breast cancer patients undergoing radiotherapy range from 1.8% to 19% (Pierce et al., 1992). Animal studies have shown that exposure to ionizing radiation appears to stimulate bone loss as an acute response, with early trabecular bone loss occurring during the first week of radiation (Willey et al., 2010). Lane et al. (2006), reported that patients with radiation-induced fractures had decreased levels of bone density, and a further study reported impaired bone formation and decreased osteoblast proliferation and differentiation following radiotherapy. Additionally, increased numbers of osteoclasts have been detected within the proximal tibial metaphysis after exposure to radiation; implying the involvement of osteoclasts (Willey et al., 2010). As osteoporosis typically reflects an imbalance between bone resorption and formation, current therapies and agents used for treating osteoporosis either inhibit bone resorption or stimulate bone formation, and also stimulate the recovery of bone mass and bone metabolism. Herbal drugs and their extracts have recently received great attention due to their potential inhibitory effects on the radiation-induced osteoporosis. The plant *Panax notoginseng* (Burk.) F.H. Chen belongs to the family *Araliaceae*, and since ancient times has been widely used in traditional Chinese herbal medicine to promote bone healing following a fracture (Qiang et al., 2010). *P. notoginseng* saponins (PNS) are pharmacologically active molecules which have been shown to improve bone strength and trabecular microarchitecture, and promote bone mineral density in ovariectomized rats (Shen et al., 2014). Additionally, the balance between osteogenic differentiation and adipogenic differentiation in BMSCs has been shown to play an important role in osteoporosis (Moerman et al., 2004), and PNS have been shown to increase the proliferation of bone marrow stem cells (BMSCs) (Li et al., 2011). Such findings suggest potential therapeutic

* Corresponding author. Tel.: 86057187071625; fax: 86057187071625.
E-mail address: yinliming2015@yeah.net (Y. Liming).
[1] These authors contributed equally to this work

http://dx.doi.org/10.1016/j.phymed.2015.05.056
0944-7113/

uses for PNS in conditions such as bone nonunion, osteoporosis, and osteonecrosis (Li et al., 2011). However, the effects of PNS on radiation-induced osteoporosis and their mechanism of action remain unclear. Furthermore, previous studies investigating the therapeutic effects of *P. notoginseng* have focused on the saponins found in its roots, and the pharmacological effects of saponins derived from other parts of the plant such as the leaves have not been studied. We conducted this study to examine the effects of total saponins derived from the leaves of *P. notoginseng* (LPNS) in a mouse model of radiation-induced osteoporosis. We also investigated the effects of LPNS on the differentiation and activation of osteoblasts and osteoclasts *in vitro* with the goal of understanding their mechanism of action.

Material and methods

Preparation of LPNS

Total saponins derived from the leaves of *P. notoginseng*, and which satisfied criteria in the Pharmacopoeia of the People's Republic of China 2010 were purchased from Wen Shan (Kunming, China). Nine substances used as chemical standards (ginsenoside Rg1, Rb1, Rc, Rb2, Rb3, 20(S)-F1, Rd, 20(S)-F2 and 20(S)-Rg3) were purchased from the National Institute for Pharmaceutical and Biological Products (Beijing, China). A fingerprint analysis of the LPNS preparation was performed as described by Ningna et al., (2014). The LPNS fingerprints (Fig. S1) were characterized by two dominant peaks of ginsenoside Rc (peak 3) and ginsenoside Rb3 (peak 5), with much lower contents of ginsenoside Rg1 (peak 1), ginsenoside Rb1 (peak 2), ginsenoside Rb2 (peak 4), ginsenoside 20(S)-F1 (peak 6), ginsenoside Rd (peak 7), ginsenoside 20(S)-F2 (peak 8) and ginsenoside 20(S)-Rg3 (peak 9). The other peaks were also identified by using mass spectrometry (data not shown). It was found that peak *a, d, e, f* and *g* were diol saponins, and peak *b* was triol saponins. Therefore, the total saponins in the extracts were 79.22%. The relative contents of these compounds in LPNS were calculated as the peak area of each compound relative to the total peak area, respectively (Table S1). The animal studies were conducted using LPNS dissolved in distilled water.

Establishment of a radiation-induced osteoporosis mouse model

Male BALB/c wild type mice were purchased from the Institutional Animal Center (Shanghai, China). All animal studies were conducted in compliance with guidelines published by the Institutional Animal Care and Use Committee of Zhejiang Chinese Medical University, China. Food and water were available *ad libitum*.

Irradiation studies were performed using the protocol described by Hamilton et al., 2006. Briefly, 50 mice were randomized to five groups ($n = 10$ mice per group). Groups 1–4 groups received whole body irradiation with 60-Cobalt gamma rays (Zhejiang Academy of Agricultural Science, Hangzhou, China) administered at a rate of 1.0 Gy/min for 8 min (sublethal doses). The mice in group 5 were not irradiated. Three days after irradiation, mice in each of the four irradiated groups were orally administered a solution containing LPNS (either 0, 50, 100 or 200 mg/kg.day, respectively) dissolved in distilled water for 15 consecutive days. The non-irradiated mice received distilled water without LPNS.

Following the last administration of distilled water or LPNS solution, the mice were anesthetized with chloral hydrate (300 mg/kg, i.p.) (Sinopharm®, Beijing, China) and blood samples were withdrawn from the femoral artery. The blood samples were allowed to clot and then centrifuged at 3000 g for 10 min to the isolate serum fractions. Samples of bone marrow for use in FACS analyses were collected in heparin coated anticoagulant tubes. The bilateral femurs of each mouse were dissected, and the cells were used for conducted CFU-F assays and real-time reverse transcription-PCR studies.

Detection of bone mineral density

Mice were scanned using quantitative micro-computed X-ray tomography as described by Rana et al. (2012). Next, data obtained from studies of the bilateral femurs were used for determination of bone mineral densities using Scanco evaluation software (Scano Medical, Switzerland).

Fibroblast colony-forming unit (CFU-F) assays

Bone marrow cells were collected from the bilateral femurs of mice, and used in conducting CFU-F assays as previously described by Yin et al., (2013). Briefly, 10^6 cells were cultured for 7 days. The cells were stained with Giemsa stain, and the colony forming units were counted under a microscope. A CFU-F was defined as a mass produced by $\geq$ 50 fibroblasts.

Alkaline phosphatase (AKP) activity assay

The activities of alkaline phosphatase (AKP) from mouse sera or BMSCs were both analyzed by using commercial kits (Nanjing Jiancheng Biological Product, Nanjing, China). Levels of alkaline phosphatase (AKP) in mouse sera were determined using an automatic analyzer (Beckman-Coulter CX-7; Beckman-Coulter; Brea, CA, USA). The AKP activities of cells formed from BMSCs following treatment with LPNS (0, 50, 100 or 200 mg/l) for 3 days were assessed as previously described (Li et al., 2011).

Cell culture and differentiation

Bone marrow mesenchymal stem cells (BMSCs) were isolated using the protocol of Yin et al, (2013), and bone marrow mononuclear cells (BMNCs) were isolated as described by Zeng et al., (2006). For the differentiation of BMSCs into osteoblasts, BMSCs were cultured at a density of 1×10^4 cells/cm^2 in osteogenic induction medium (Cyagen Biosciences; Santa Clara, CA, USA) and simultaneously treated with LPNS at concentrations of 0, 50, 100 or 200 mg/l. Biological characteristics of the cells were then examined using MTT assays, AKP activity assays, Alizarin Red S staining, and western-blotting, respectively.

For differentiation of BMNCs into osteoclasts, BMNCs were cultured for 7 days in medium containing macrophage colony-stimulating factor (M-CSF; 10 ng/ml), RANKL (50 ng/ml) (Reprotech; Rocky Hill, NJ, USA), and LPNS (0, 50, 100 or 200 mg/l). The cells were then harvested for FACS analysis, TRAP staining, determination of bone resorption activity, and analysis by real-time reverse transcription-PCR, respectively.

MTT assay

BMSCs were induced to differentiate into osteoblasts (see above) by treatment with LPNS (0, 50, 100 or 200 mg/l) for 24 h, 48 h, or 72 h, respectively. Next, cell viability was assayed as described (Li et al., 2011).

Alizarin Red S staining

BMSCs were induced to differentiate into osteoblasts (see above) by 7 days of treatment with LPNS (0, 50, 100 or 200 mg/l). Mineralization in the induced osteoblasts was determined by Alizarin Red S staining as previously described (Li et al., 2011). The mineral nodes were detected by microscopic examination.

Western blotting

Aliquots of osteoblasts (~10^6) which had differentiated from BMSCs by treatment with LPNS (0, 50, 100 or 200 mg/l) for 7 days were collected. The protein levels of RUNX and OPG were determined by western blotting as described before (Li et al., 2011). The staining intensities of the protein bands were measured, quantified, and normalized against staining of beta-actin using Quantity One software (Bio-Rad Laboratories; Hercules, CA, USA). The primary antibodies for RUNX, OPG, and beta-actin (the species-reactivities of these antibodies are both mouse, and the catalog numbers are sc-8564, sc-8468 and sc-47778, respectively) were purchased from Santa Cruz Biotechnology; Santa Cruz, CA, USA and diluted 1:1000.

Flow cytometry analysis

Cells were washed twice by phosphate buffered solution (PBS) and then incubated with either isotypic control or monoclonal antibodies against PE-CD45, FITC-CD71, FITC-CD117, APC-CD115, and APC-RANKL (receptor activator of nuclear factor κB ligand) for 30 min on ice in the dark, respectively. The incubated cells were then washed twice with cold Hank's Balanced Salt Solution (HBSS) and analyzed by flow cytometry. The antibodies used for flow cytometry were purchased from eBioscience (San Diego, CA, USA).

Levels of cytokines IL-2, IL-4, IL-6, INFγ, TNFα, IL-17, and IL-10 in the serum of mouse were detected by using BD Cytometric Bead Array (CBA) Mouse Th1/Th2/Th17 Cytokine Kit (BD Biosciences, San Jose, CA, USA) according to the manufacturer's instruction (Catalog Number: 560485), as described previously (Perl et al., 2005). Briefly, 50 μl of mouse inflammation capture bead suspension and 50 μl of the Mouse Th1/Th2/Th17 PE detection reagent mixed with 50 μl of sample or standard dilutions and incubated for 2 h at room temperature in the dark. The data were analyzed on a FCAP Array software (BD Biosciences, San Jose, CA, USA) according to the manufacturer's instruction.

Tartrate-resistant acid phosphatase (TRAP) staining

TRAP staining was conducted using a commercially available staining kit (Sigma-Aldrich, St. Louis, Mo, USA). Briefly, after removing the culture medium and washing one time with 100 μl of PBS, 50 μl of 10% formalin neutral buffer solution was added to each well of the culture dish and let stand for 5 min at room temperature. Next, the wells were washed 3 times and the residual contents were reacted with 1 vial of chromogenic substrate mixed with 5 ml of tartrate-containing buffer. Next, 50 μl of chromogenic substrate was added to each well, and the osteoclasts were observed under a microscope (Rana et al., 2012).

Assessment of bone resorption activity of osteoclasts

Aliquots of osteoblasts (~10^2) which had differentiated from BMSCs by treatment with LPNS (0, 50, 100 or 200 mg/l) for 7 days were layered onto cortical bone slices (Nordic Bioscience, Denmark) and co-culturing for 48 h. The slices were then fixed with glutaraldehyde, stained with toluidine blue, and areas showing bone resorption were identified by microscopy. The areas showing bone resorption were analyzed using Image Pro-Plus software (Media Cybernetics; Rockville, MD, USA).

RNA preparation and real-time reverse transcription-PCR

Total RNA was isolated using TRIzol® LS Reagent (Invitrogen Corp., Carlsbad, CA, USA) according to the manufacturer's instructions (Jiang et al., 2014). The Ct (cycle threshold) values were normalized to the expression levels of β-actin. The primers used in this study are shown in Table 1.

Table 1
Primers used in study.

Gene	Forward (5′-3′)	Reverse (5′-3′)
Runx2	TTTAGGGCGCATTCCTCATC	TGTCCTTGTGGATTAAAAGGACTTG
TRAP	GGCTACTTGCGGTTTCACTAT	CCTTGGGAGGCTGGTCT
OPG	GTGGTGCAAGCTGGAACCCCAG	AGGCCCTTCAAGGTGTCTTGGTC
Atp6i	ATGTTCCGGAGTGAAGAGGTG	TCCTGGATGCGCAGCAGFIGGTC

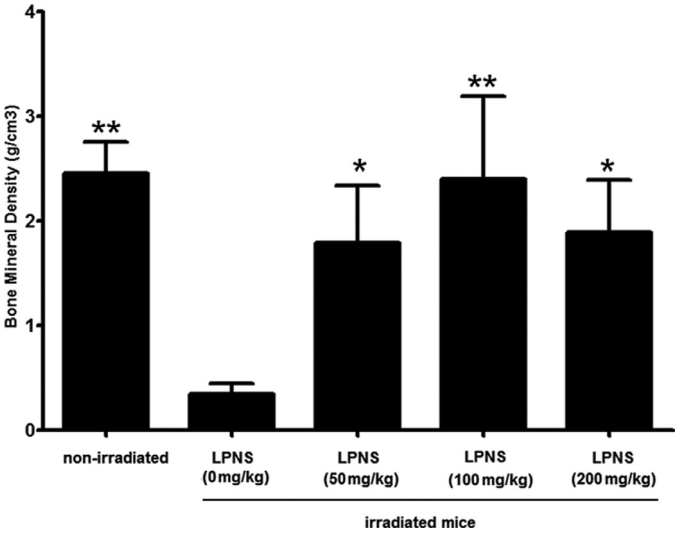

Fig. 1. Effects of LPNS on bone mineral density in radiation-induced osteoporosis mice model. Values are means ± SEM ($n = 10$). **, $p < 0.01$; *, $p < 0.05$; compared with the group of 0 mg/kg·day.

Statistical analysis

All data are expressed as the mean ± standard error of the mean (SEM) and were analyzed using the *t*-test or one-way analysis of variance (ANOVA). The non-parametric single sample Wilcoxon test was used for analysis of qRT-PCR results. *P*-values < 0.05 were considered statistically significant ($^*P < 0.05$, $^{**}P < 0.01$). All experiments were performed a minimum of three times.

Results

LPNS suppressed radiation-induced osteoporosis in vivo

Our results showed that the mean value for bone mineral density (BMD) in irradiated mice was 85.7% lower compared to that in non-irradiated mice (0.35 ± 0.10 versus 2.45 ± 0.30 g/cm^3; $P < 0.01$; Fig. 1). However, after 15 days of dosing with LPNS (50, 100 or 200 mg/kg.day) the mean values for bone mineral density in these three groups of irradiated mice increased by 80.4% ($P < 0.05$), 85.4% ($P < 0.01$) and 81.5% (P < 0.05), respectively, when compared with the bone density in irradiated mice which had not received LPNS (Fig. 1).

Bone formation was accelerated by LPNS in vivo

When compared with the non-irradiated mice, irradiated mice showed significantly decreased numbers of CFU-Fs ($P < 0.01$; Fig. 2A) and serum levels of AKP ($P < 0.01$; Fig. 2B). Furthermore, the mRNA levels for osteoprotegerin and RUNX2 in the bone marrows from irradiated mice were significantly lower than those in the non-irradiated mice (both *P*-values < 0.05; Fig. 2C). However, irradiated mice which had received oral LPNS at a dose of 100 mg/kg.day showed increases in their numbers of CFU-Fs (8.33 ± 2.11 versus 1.67 ± 0.08, $P < 0.01$; Fig. 2A), serum AKP levels (2103.27 ± 181.90 versus 1212.67 ± 142.03, $P < 0.01$; Fig. 2B), and mRNA levels for osteoprotegerin and RUNX2

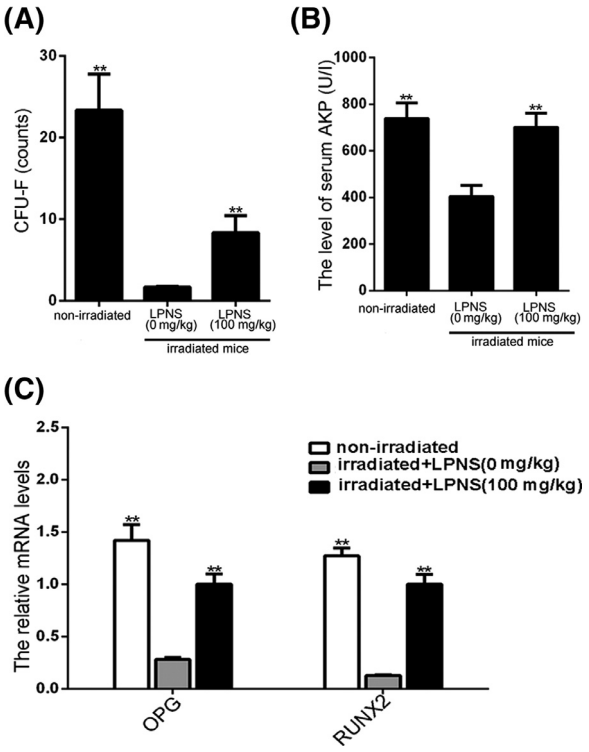

Fig. 2. Effects of LPNS on the bone formation in radiation-induced osteoporosis mice model. (A) The numbers of CFU-Fs. (B) The levels of serum AKP. (C) The mRNA levels of OPG and RUNX2. Values are means ± SEM ($n = 10$). **, $p < 0.01$; compared with the group of 0 mg/kg·day.

($P < 0.01$, respectively; Fig. 2C) when compared to mice which had not received LPNS.

Bone resorption was suppressed by LPNS in vivo

When compared to non-irradiated mice, the irradiated mice showed significantly fewer numbers of $CD117^+$ cells ($P < 0.01$; Fig. 3). In contrast, the numbers of $CD117^+/RANKL^+$ cells and $CD71^+/CD115^+$ cells were significantly increased in the irradiated mice ($P < 0.05$ and $P < 0.01$, respectively) (Fig. 3), and the mRNA levels for TRAP and ATP6i were also increased (both P-values < 0.01; Fig. 4). When compared with the irradiated mice which had not received LPNS, the numbers of $CD117^+$ cells were significantly higher (1.31 ± 0.65 versus 5.42 ± 0.33, $P < 0.01$; Fig. 3) but the numbers of $CD117^+/RANKL^+$ cells and $CD71^+/CD115^+$ cells were significantly lower in irradiated mice which had received LPNS (37.70 ± 8.1 versus 14.48 ± 5.3; $P < 0.05$) and (2.20 ± 0.34 versus 0.44 ± 0.11; $P < 0.05$), respectively (Fig. 3). The mRNA levels for TRAP and ATP6i were also significantly decreased by LPNS treatment (both P-values < 0.05; Fig. 4).

Inflammation was weakened by LPNS in vivo

The data showed that LPNS decreased the levels of IFN-γ, TNF-α, IL-6, and IL-17 which had been previously significantly increased by irradiation ($P < 0.05$, $P < 0.01$, $P < 0.01$, $P < 0.01$, respectively; Table 2). Moreover, LPNS increased the levels of IL-10 ($P < 0.05$, Table 2), but showed no effects on IL-4 and IL-2 in the irradiated mice when compared with IL-4 and IL-2 levels in irradiated mice which had not received LPNS (Table 2).

LPNS promoted differentiation of BMSCs into osteoblasts in vitro

BMSCs were cultured in osteogenic induction medium and simultaneously treated with various concentrations of LPNS (0, 50, 100, and 200 mg/l). Compared to cells cultured without LPNS, cells cultured with 50, 100 or 200 mg/l LPNS demonstrated increased proliferation (Fig. 5A), increased AKP activities ($P < 0.05$, $P < 0.01$, $P < 0.01$, respectively; Fig. 5B), increased levels of both RUNX2 protein ($P < 0.05$, $P < 0.01$, $P < 0.01$, respectively; Fig. 6A and B) and OPG protein ($P < 0.05$, $P < 0.01$, $P < 0.05$, respectively; Fig. 6A and B), as well as increased calcium nodule formation (Fig. 5C).

Table 2
Levels of inflammatory factors.

	Non-irradiated	Irradiated + LPNS(0 mg/kg.day)	Irradiated + LPNS(100 mg/kg.day)
IFN-γ	8.48 ± 2.43	15.69 ± 6.87	10.30 ± 3.64*
TNF-α	21.79 ± 4.01	62.99 ± 16.41	28.74 ± 13.22**
IL-6	7.44 ± 2.10	14.77 ± 4.99	9.89 ± 3.47**
IL-17	5.79 ± 0.28	8.02 ± 0.50	4.91 ± 0.56**
IL-10	29.60 ± 4.46	14.19 ± 4.77	37.04 ± 7.81*
IL-4	4.51 ± 0.39	3.12 ± 0.66	4.16 ± 1.28
IL-2	5.14 ± 0.72	5.62 ± 0.87	4.81 ± 1.09

Effects of LPNS on the inflammation factors in radiation-induced osteoporosis mice model. Values are means ± SEM ($n = 10$).
* $P < 0.05$.
** $P < 0.01$; compared with the group of 0 mg/kg.day.

LPNS promoted differentiation of BMNCs into osteoclasts precursor cells but had no effect on activation of osteoclasts in vitro

Following treatment of BMNCs with the medium containing M-CSF(10 ng/ml), RANKL (50 ng/ml) and LPNS (50, 100 or 200 mg/l), flow cytometry analyses showed increased numbers of $CD45^+/CD71^+/CD115^+$ cells ($P < 0.05$, $P < 0.01$, $P < 0.01$, respectively; Fig. 7), while such increases were not seen in BMNCs cultured without LPNS. But LPNS did not affect the levels of TRAP and ATP6i (data not shown), the staining of TRAP (Fig. 8A) or bone resorption activity (Fig. 8B) in differentiated osteoclasts.

Discussion

P. notoginseng has been used since ancient times to treat bone fractures in China, and *P. notoginseng* saponins (PNS) are the major pharmacologically active constituents of *P. notoginseng*. PNS have been shown to suppress ovariectomy-induced decreases in bone mineral density, bone mechanical strength, and bone microarchitectural structure without having a hyperplastic effect on the uterus (Shen et al., 2010). PNS were also shown to protect rabbit bone marrow stromal cells from oxidative stress-induced damage and apoptosis (Qiang et al., 2010). However, the effects of total saponins found in the leaves of *P. notoginseng* (LPNS) on radiation-induced osteoporosis and its intrinsic mechanism have not been well documented. In our present study, we assessed the effects of LPNS in a radiation-induced mouse model of osteoporosis and found that LPNS suppressed radiation-induced osteoporosis by regulating bone formation and resorption. Additionally, this study confirmed that radiation could induce osteoporosis.

Rana et al., (2012) reported that mice lacking Nrf2 exhibited greater bone loss after radiation exposure compared to wild-type mice, in which the bone volumes remained unchanged. However, Hamilton et al., (2006) reported significant bone loss in 9-week-old mice. Such seemingly contradictory data may result from different sources of radiation being used in different studies. The current study utilized only one dose of radiation ($^{60}Co\gamma$; 1.0 Gy/min, 8 min), and showed it produced a significant decrease in the bone mineral density of irradiated mice, which was in agreement with results in a previous study (Hamilton et al., 2006). Additionally, administration of LPNS significantly reversed the decrease in bone mineral density. With regard to bone metabolic markers, both bone formation and the bone resorption index were used to investigate possible

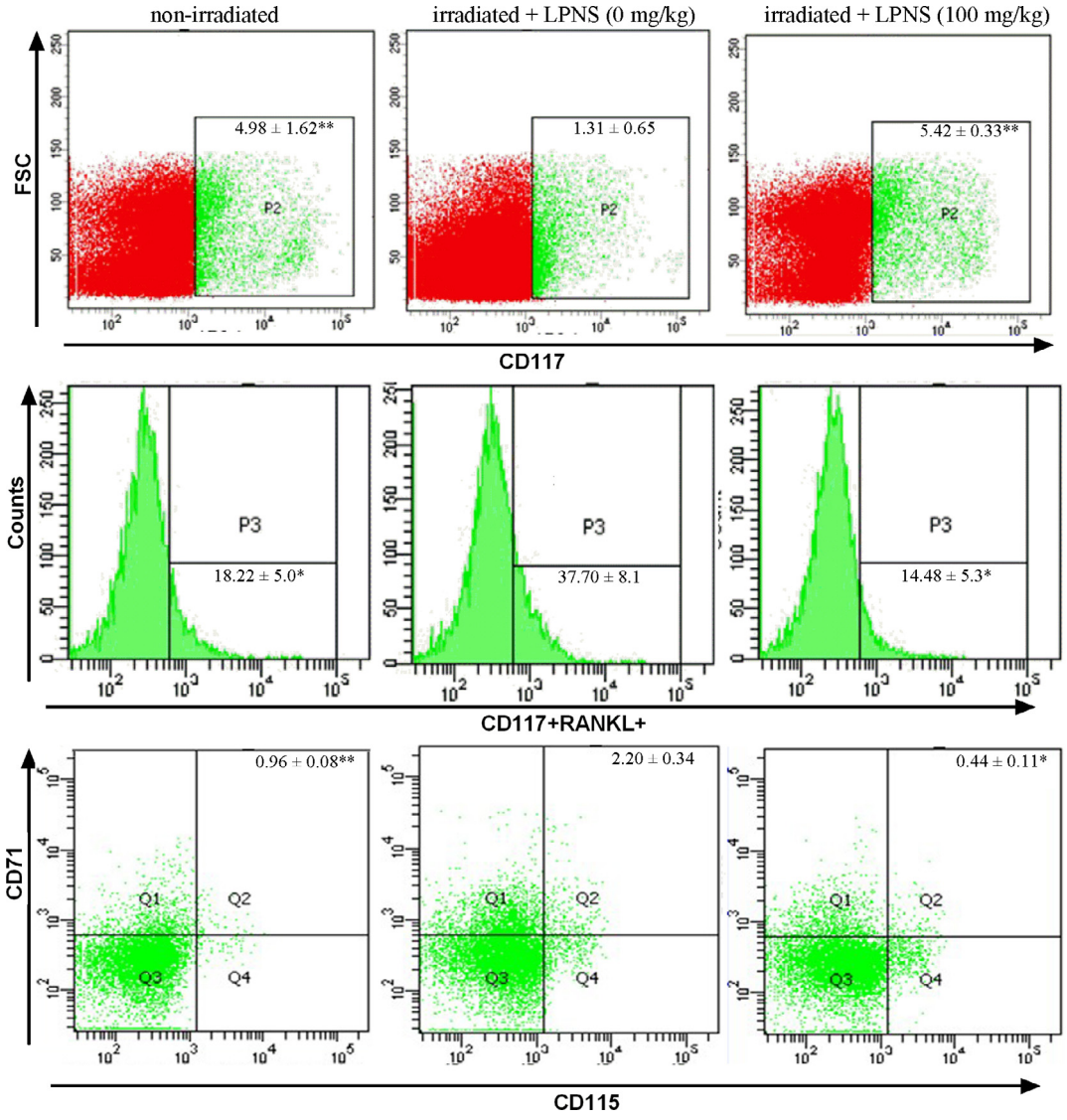

Fig. 3. Effects of LPNS on the progenitors ($CD117^+$ cells) and precursors ($CD117^+/RANKL^+$ cells and $CD71^+/CD115^+$ cells) of osteoclasts in radiation-induced osteoporosis mice model. Values are means ± SEM ($n = 10$). **, $p < 0.01$; *, $p < 0.05$; compared with the group of 0 mg/kg·day. FSC, forward scatter; Counts, the number of cells.

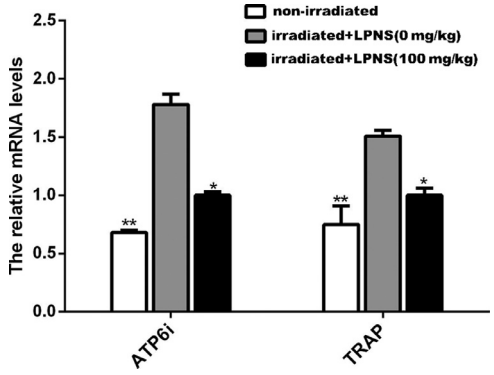

Fig. 4. Effects of LPNS on the mRNA levels of ATP6i and TRAP in radiation-induced osteoporosis mice model. Values are means ± SEM ($n = 10$). **, $p < 0.01$; *, $p < 0.05$; compared with the group of 0 mg/kg·day.

mechanisms of LPNS activity. AKP activity is recognized as an important marker of bone formation (Zhang et al., 2009), and our data showed that LPNS improved serum AKP activity in the irradiated mice. CFU-F numbers, which reflect the numbers of circulating osteoblast precursors, were also increased by LPNS. Additionally, the mRNA levels for RUNX2 (an osteoblast-specific transcription factor) and osteoprotegerin (a RANKL antagonist) were elevated by LPNS. This indicated that bone formation in the radiation-induced osteoporosis mouse model was accelerated by LPNS. Furthermore, our results showed that the numbers of $CD117^+$ cells, which are considered to be osteoclast progenitor cells (Jacome-Galarza et al., 2013), were increased in the irradiated mice by administration of LPNS. However, the numbers of $CD71^+/CD115^+$ cells and $CD117^+/RANKL^+$ cells, which are considered to be osteoclast precursor cells (Jacquin et al., 2006), were reduced by LPNS administration. These results indicate that while LPNS increased the numbers of osteoclasts progenitor cells, it inhibited their subsequent differentiation into osteoclast precursor cells. Moreover, LPNS decreased the mRNA levels of TRAP and ATP6i, which are classic markers of bone resorption. Levels of both TRAP and ATP6i were significantly increased in the irradiated mice, further suggesting that LPNS inhibited bone resorption in radiation-induced osteoporotic mice.

Bone homeostasis is maintained by the synchronous differentiation of osteoblasts and activation of osteoclasts, and a change in this balance of activity can result in pathologic changes in the bone. A decreased number osteoblasts and an abnormally high level of osteoclast activity can result in bone loss. We directly detected the effects of LPNS on the differentiation of BMSCs and BMNCs into osteoblasts

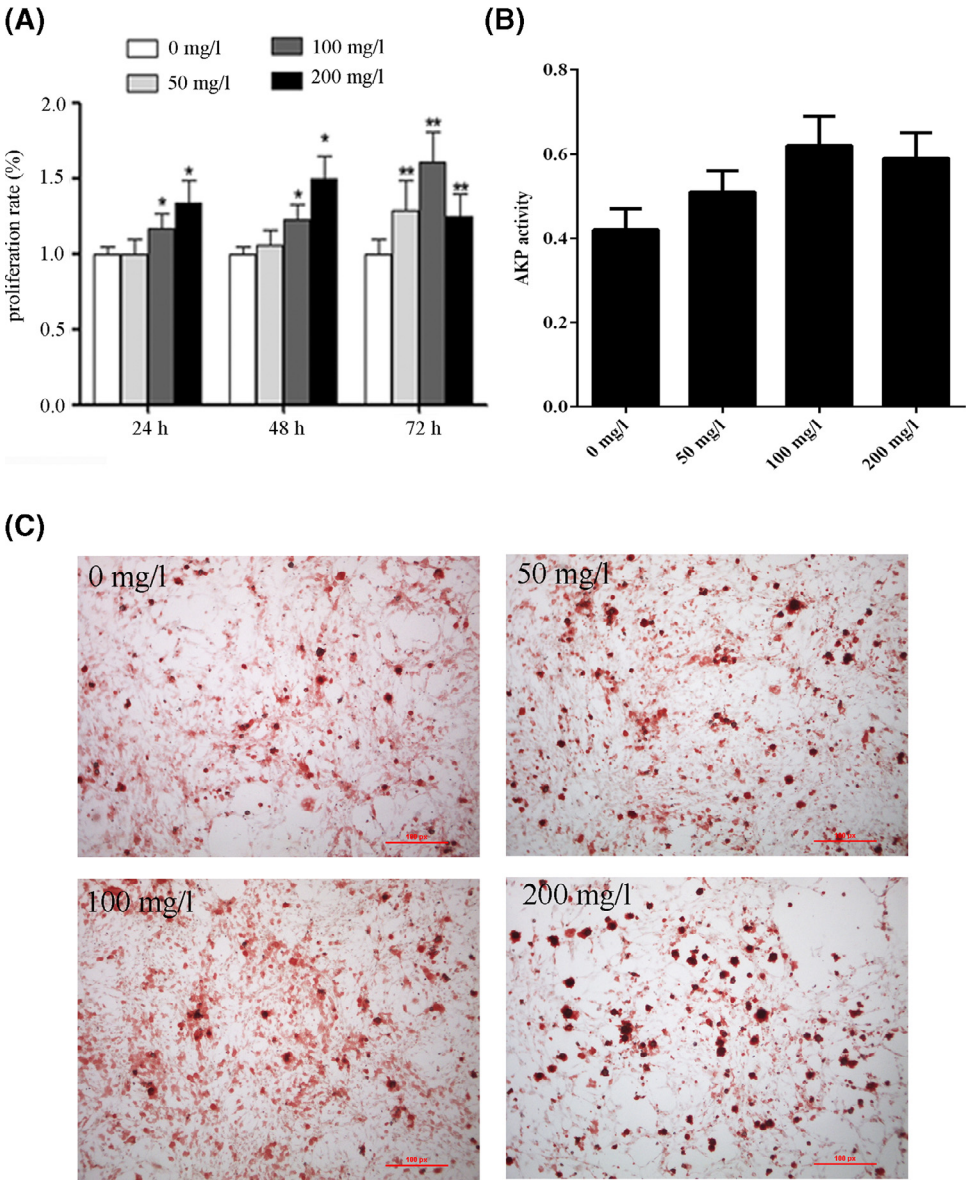

Fig. 5. Effects of LPNS on the differentiation of BMSCs into osteoblasts *in vitro*. BMSCs were cultured in osteogenic induction medium and simultaneously treated with various concentrations of LPNS (0, 50, 100, and 200 mg/l). (A) The proliferation rate was assessed after 24, 48 and 72 h by MTT assay. The activities of AKP (B) and the Alizarin Red S staining(C) were assessed in the cells formed from BMSCs following treatment with LPNS. Values are means ± SEM. **, $p < 0.01$; *, $p < 0.05$; compared with the group of 0 mg/l.

and osteoclasts, respectively. We found that LPNS promoted BMSC proliferation and also increased both AKP activity, and the levels of RUNX2 and OPG. Additionally, LPNS increased calcium nodule formation in the differentiated cells. On the other hand, flow cytometry analyses showed increased numbers of $CD45^+/CD71/^+CD115^+$ cells following administration of LPNS. LPNS did not affect the levels of TRAP and ATP6i, the staining of TRAP, or the bone resorption activity shown by differentiated osteoclasts. These findings indicate that while LPNS significantly increased the numbers of osteoclast precursor cells, it had no effect on the bone resorption capacity of osteoclasts. These *in vitro* findings suggest that LPNS exerts antiosteoporotic effects by regulating the balance between bone formation and resorption.

P. notoginseng saponins have been shown to produce a myriad array of pharmacological effects, including anti-oxidative and anti-inflammatory responses (Ningna et al., 2014). Inflammation is believed to play an important role in radiation-induced responses (Zhao and Robbins, 2009). In the present study, we found that exposure to radiation increased the levels of IFN-γ, TNF-α, IL-6, and IL-17, and decreased the levels of IL-10. IL-10 is a negative regulator of inflammatory cascades which inhibit bone resorption (Hong et al., 2000), while the other four factors are positive regulators which are capable of stimulating osteoclastic bone resorption (Abdelmagid et al., 2014). Furthermore, we found that LPNS decreased the levels of the four positive regulators and increased the levels of a negative regulator. The levels produced by LPNS might be involved in the impaired bone resorption caused by radiation. However, when compared with the irradiated mice which had not received LPNS, the levels of IL-2 still showed a non-significant decreasing trend but the levels of IL-4 showed a non-significant increasing trend in irradiated mice which had received LPNS. IL-4 is an anti-osteoclastogenic factor which is generated by T cells (D'Amelio et al., 2008a), while IL-2 is one of the main reasons of decreased bone mineral density and bone formation (Abdelmagid et al., 2014). Therefore, the sample size of the radiation-induced mice model will be expanded, and the effects of LPNS on the levels of IL-2 and IL-4 still to be investigated in the future study.

In conclusion, we demonstrated that LPNS can reverse osteoporosis in a radiation-induced mouse model, and that LPNS exhibits

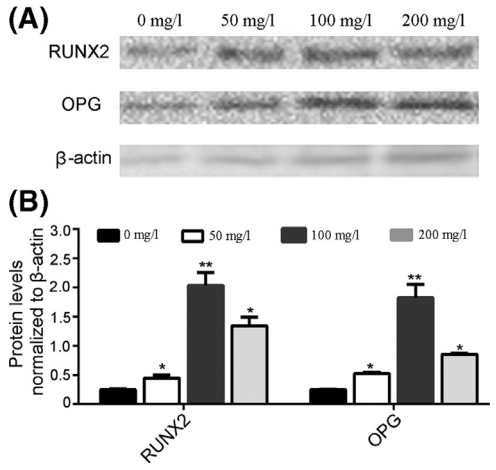

Fig. 6. Effects of LPNS on the protein levels of RUNX2 and OPG in the cells formed from BMSCs following treatment with LPNS (0, 50, 100 and 200 mg/l). (A) Representative western blot of RUNX2 and OPG. (B) Quantification (fold changes) of the Western blots. Values are means ± SEM. **, $p < 0.01$; *, $p < 0.05$; compared with the group of 0 mg/l.

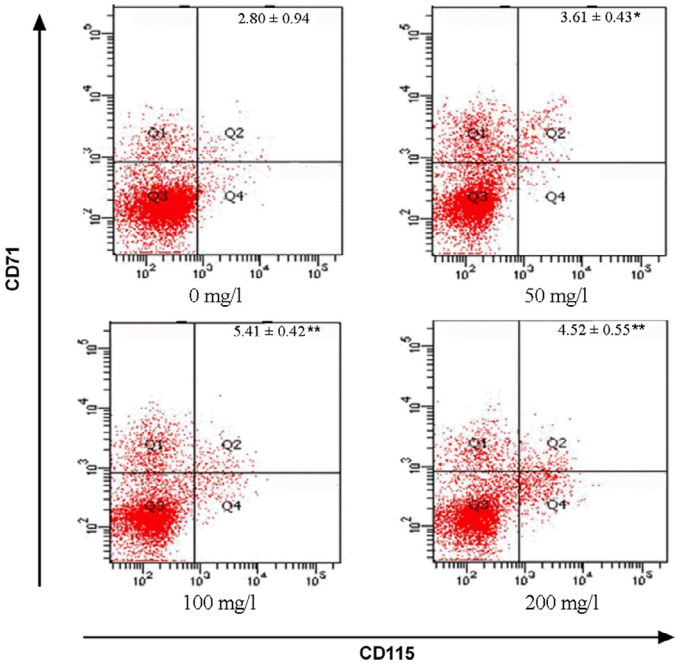

Fig. 7. Effects of LPNS on the $CD45^+/CD71^+/CD115^+$ cells following treatment of BMNCs with the medium containing M-CSF (10 ng/ml), RANKL (50 ng/ml) and LPNS (0, 50, 100 or 200 mg/l). Values are means ± SEM. **, $p < 0.01$; *, $p < 0.05$; compared with the group of 0 mg/l.

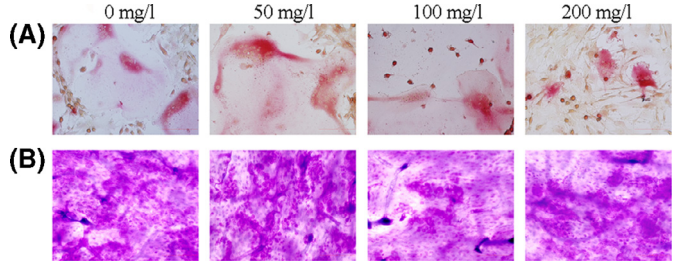

Fig. 8. Effects of LPNS on the staining of TRAP (A) or bone resorption activity (B) in the cells following treatment of BMNCs with the medium containing M-CSF(10 ng/ml), RANKL (50 ng/ml) and LPNS (0, 50, 100 or 200 mg/l).

potential antiosteoporotic properties when tested in osteoblasts and osteoclasts *in vitro*. These results suggest the total saponins extracted from the leaves of *Panax notoginseng* (a traditional Chinese medicinal plant), warrant further investigation as a potential agent to treat radiation-induced osteoporotic disease.

Conflict of interest

The authors declare that they have no conflict of interest.

Supplementary Materials

Supplementary material associated with this article can be found, in the online version, at doi:10.1016/j.phymed.2015.05.056.

References

Abdelmagid, S.M., Barbe, M.F., Safadi, F.F., 2015. Role of inflammation in the aging bones. Life Sci. 123, 25–34.
D D'Amelio, P., Grimaldi, A., Bella, S., 2008. Estrogen deficiency increases osteoclastogenesis upregulating T cells activity: a key mechanism in osteoporosis. Bone 43, 92–100.
Hamilton, S.A., Pecaut, M.J., Gridley, D.S., Travis, N.D., Bandstra, E.R., Willey, J.S., Nelson, G.A., Bateman, T.A., 2006. A murine model for bone loss from therapeutic and space-relevant sources of radiation. J. Appl. Physiol. 101, 789–793.
Jacome-Galarza, C.E., Lee, S.K., Lorenzo, J.A., Aguila, H.L., 2013. Identification, characterization, and isolation of a common progenitor for osteoclasts, macrophages, and dendritic cells from murine bone marrow and periphery. J. Bone Miner. Res. 28, 1203–1213.
Jacquin, C., Gran, D.E., Lee, S.K., Lorenzo, J.A., Aguila, H.L., 2006. Identification of multiple osteoclast precursor populations in murine bone marrow. J Bone Miner Res 21, 67–77.
Jiang, J., Li, J., Jia, X., 2014. The antiosteoporotic activity of central-icaritin (CIT) on bone metabolism of ovariectomized rats. Molecules 19, 18690–18704.
Lane, J.M., Serota, A.C., Raphael, B., 2006. Osteoporosis: differences and similarities in male and female patients. Orthop. Clin. North Am. 37, 601–609.
Li, X.D., Wang, J.S., Chang, B., Chen, B., Guo, C., Hou, G.Q., Huang, D.Y., Du, SX, 2011. Panax notoginseng saponins promotes proliferation and osteogenic differentiation of rat bone marrow stromal cells. J. Ethnopharmacol. 134, 268–274.
Hong, M.H., Williams, H., Jin, C.H, Pike, J.W., 2000. The inhibitory effect of interleukin-10 on mouse osteoclast formation involves novel tyrosine-phosphorylated proteins. J. Bone Min. Res. 15, 911–918.
Moerman, E.J., Teng, K., Lipschitz, D.A., Lecka-Czernik, B., 2004. Aging activates adipogenic and suppresses osteogenic programs in mesenchymal marrow stroma/stem cells: the role of PPAR-gamma2 transcription factor and TGF-beta/BMP signaling pathways. Aging Cell 3, 379–389.
Ningna, Z., Yang, T.G., Richard, F.K., Xiaoxia, M., Jianming, X., 2014. Antioxidative effects of Panax notoginseng saponins in brain cells. Phytomedicine 21, 1189–1195.
Perl, M., Chung, C.S., Lomas, Neira, J., Rachel, TM., Biffl, W.L., Cioffi, W.G., Ayala, A., 2005. Silencing of Fas, but not caspase-8, in lung epithelial cells ameliorates pulmonary apoptosis, inflammation, and neutrophil influx after hemorrhagic shock and sepsis. Am. J. Pathol. 167, 1545–1559.
Pierce, S.M., Recht, A., Lingos, T.I., Abner, A., Vicini, F., Silver, B., Herzog, A., Harris, J.R., 1992. Long-term radiation complications following conservative surgery (CS) and radiation therapy (RT) in patients with early stage breast cancer. Int. J. Radiat. Oncol. Biol. Phys. 23, 915–923.
Qiang, H., Zhang, C., Shi, Z.B., Yang, H.Q., Wang, K.Z., 2010. Protective effects and mechanism of Panax Notoginseng saponins on oxidative stress-induced damage and apoptosis of rabbit bone marrow stromal cells. Chin. J. Integr. Med. 16, 525–530.
Rana, T., Schultz, M.A., Freeman, M.L., Biswas, S., 2012. Loss of Nrf2 accelerates ionizing radiation-induced bone loss by upregulating RANKL. Free Radic. Biol. Med. 53, 2298–2307.
Shen, Y., Li, Y.Q., Li, S.P., Ma, L., Ding, L.J., Ji, H., 2010. Alleviation of ovariectomy-induced osteoporosis in rats by Panax notoginseng saponins. J. Nat. Med. 64, 336–345.
Willey, J.S., Livingston, E.W., Robbins, M.E., Bourland, J.D., Tirado-Lee, L., Smith-Sielicki, H., Bateman, T.A., 2010. Risedronate prevents early radiation-induced osteoporosis in mice at multiple skeletal locations. Bone 46, 101–111.
Williams, H.J., Davies, A.M., 2006. The effect of X-rays on bone: a pictorial review. Eur. Radiol. 16, 619–633.
Yin, L.M., Jiang, H.f., Wang, X., Qian, X.D., Gao, R.L., Lin, X.J., Chen, X.H., Wang, L.C., 2013. Effects of sodium copper chlorophyllin on mesenchymal stem cell function in aplastic anemia mice. Chin. J. Integr. Med. 19, 360–366.
Zeng, L., Yang, S., Wu, C., Ye, L., Lu, Y., 2006. Effective transduction of primary mouse blood- and bone marrow-derived monocytes/macrophages by HIV-based defective lentiviral vectors. J. Virol. Meth. 134, 66–73.
Zhang, R., Liu, Z., Li, C., Hu, S., Liu, L., Wang, J., Mei, Q., 2009. Du-Zhong (Eucommiaulmoides Oliv.) cortex extract prevent OVX-induced osteoporosis in rats. Bone 45, 553–559.
Zhao, W., Robbins, M.E., 2009. Inflammation and chronic oxidative stress in radiation-induced late normal tissue injury: therapeutic implications. Curr. Med. Chem. 16, 130–143.